MCB
Journals.ASM.org

DGCR14 Induces *Il17a* Gene Expression through the RORγ/BAZ1B/RSKS2 Complex

Ichiro Takada

Division of Biochemistry, Department of Biomedical Sciences, Nihon University School of Medicine, Itabashi-ku, and Department of Microbiology and Immunology, School of Medicine, Keio University, Shinjuku-ku, Tokyo, Japan

The *Dgcr14/Es2* gene is located in a chromosomal region the loss of which has been associated with DiGeorge syndrome, a cause of immunodeficiency, heart defects, and skeletal abnormalities. However, the role of DGCR14 protein remains to be elucidated. Here, I found that DGCR14 protein acts as a coactivator of RORγt in T_H17 cells. Biochemical purification of the RORγ coregulator complex allowed me to identify the associated DGCR14 protein by matrix-assisted laser desorption ionization–time of flight mass spectrometry. Overexpression of *Dgcr14* mRNA enhanced RORγt-mediated transcriptional activity and facilitated T_H17 cell differentiation. Furthermore, knockdown of Dgcr14 reduced *Il17a* mRNA expression. I also found that DGCR14 associated with ribosomal S6 kinase 2 (RSK2, also called RpS6ka3) and BAZ1B, both of which were recruited to the *Il17a* promoter during T_H17 cell differentiation. Knockdown of *Baz1b* or *RpS6ka3* also reduced *Il17a* mRNA expression, and *Baz1b* knockdown increased transcriptional suppressive histone marks (histone H3K9me3) on the *Il17a* promoter. My findings showed the roles of DGCR14, RSK2, and BAZ1B in the transcriptional regulation of *Il17a* mRNA during T_H17 cell differentiation.

Retinoid-related orphan nuclear receptor gamma (RORγ, also called Rorc or Nr1f3) is a member of the nuclear hormone receptor (NR) superfamily. RORγ regulates gene transcription by binding as a monomer to specific ROR response elements (ROREs) consisting of the consensus core motif RGGTCA preceded by a 6-bp A/T-rich sequence (1). RORγ controls circadian rhythm, lymphocyte development, and lipid and glucose homeostasis. RORγ expression exhibits an oscillatory pattern (low levels during the day and maximal levels at night) in the liver, brown adipose tissue, and kidneys (2). Mice deficient in RORγ exhibit improved insulin sensitivity and glucose tolerance because of reduced hepatic gluconeogenesis, particularly during the daytime (3).

More importantly, RORγ knockout mice lack peripheral and mesenteric lymph nodes and Peyer's patches (4). Furthermore, RORγt, which is an isoform encoded by the *Rorc* gene, is highly expressed in lymphocytes and acts as a key regulator in the development of T_H17 cells (5). The N-terminal region amino acid sequence of RORγt differs from that of RORγ, but the DNA- and ligand-binding regions are conserved. RORγt knockout mice have diminished numbers of T_H17 cells and are protected against experimental autoimmune encephalomyelitis (2). Because T_H17 cells play a pivotal role in autoimmune diseases, suppression of the transcriptional activities of RORγt is critical for developing therapeutics for T_H17-mediated autoimmune disorders, including multiple sclerosis and rheumatoid arthritis. Recent studies have described the synthesis of inverse agonists of RORγ to abrogate T_H17 cell function (6–9). However, the molecular mechanism of RORγ-dependent transcriptional regulation is not fully understood.

In general, transcriptional control by NRs depends on multiprotein coregulatory complexes (10, 11). After chromatin remodeling and decreased nucleosome density, NRs bind to DNA elements. The associated transcriptional coactivators/corepressors are specific and depend on DNA elements and other transcriptional factors' context. Recent studies showed that corepressors are also necessary for recruiting coactivators (12). Moreover, the association and dissociation of coregulators constitute a transcriptional cycle (13). Thus, the identification of associated transcriptional coregulators for RORγt in $CD4^+$ T cells would be beneficial for understanding the regulation of its transcriptional activity.

Here, I purified and identified transcriptional coregulators of RORγ in T-lymphocyte-related cells. Among the identified known coregulators, I found that DGCR14 acts as a coactivator of RORγ function, although it does not have any known functional domain. I also identified proteins that associated with DGCR14. Among them, RSK2 and BAZ1B associated with DGCR14 protein on the *Il17a* promoter. These results showed the importance of the DGCR14/RSK2/BAZ1B pathway for T_H17 cell differentiation and autoimmune disease.

MATERIALS AND METHODS

Cell culture. Cells of the murine T-lymphocyte-related line 68-41 were provided by Masato Kubo (Research Center for Allergy and Immunology, Yokohama, Japan) and cultured as described previously (14). 68-41 cells were maintained in RPMI 1640 supplemented with 10% fetal bovine serum (FBS), 50 U penicillin, 50 μg ml^{-1} streptomycin, and 100 nM nonessential amino acids. For *Rorc* and *Il17a* mRNA induction, cells were stimulated with 1 μg ml^{-1} anti-CD3ε antibody in the presence or absence of 10 ng ml^{-1} recombinant interleukin-6 (IL-6; Peprotech) and 2 ng ml^{-1} transforming growth factor β (TGF-β; Peprotech) as described above. 293T cells were maintained in Dulbecco's modified Eagle's medium with 10% FBS, 50 U penicillin, and 50 μg ml^{-1} streptomycin.

Received 10 July 2014 Returned for modification 5 August 2014
Accepted 27 October 2014
Accepted manuscript posted online 3 November 2014
Citation Takada I. 2015. DGCR14 induces *Il17a* gene expression through the RORγ/BAZ1B/RSKS2 complex. Mol Cell Biol 35:344–355. doi:10.1128/MCB.00926-14.
Address correspondence to takada.ichiro@nihon-u.ac.jp.
Supplemental material for this article may be found at http://dx.doi.org/10.1128/MCB.00926-14.

doi:10.1128/MCB.00926-14

Protein purification and mass spectrometry. For RORγ complex purification, 68-41 cells were incubated with anti-CD3ε (1 μg ml^{-1}) antibody, 2 ng ml^{-1} TGF-β, and 10 ng ml^{-1} IL-6 for 8 h, after which nuclear extracts were prepared as previously described (15). Extracts were fractionated with protein G-Sepharose and eluted with 0, 100, 200, 300, 500, and 1,000 mM NaCl in buffer D (20 mM HEPES [pH 7.8], 20% glycerol, 0.2 mM EDTA, 0.2 mM phenylmethylsulfonyl fluoride [PMSF], 0.5 mM dithiothreitol [DTT]). RORγ-containing fractions (100 to 300 mM NaCl in buffer D) were collected and bound to an anti-RORγ antibody resin column prepared as previously described (16), washed with binding buffer (20 mM HEPES [pH 7.8], 250 mM KCl, 0.2 mM EDTA, 0.1% NP-40, 0.2 mM PMSF), and eluted with 0.1 M Tris-glycine (pH 3.0). After elution, proteins were separated by SDS-PAGE and then identified by matrix-assisted laser desorption ionization–time of flight mass spectrometry (MALDI-TOF MS) (Ultraflex TOF/TOF; Bruker) as previously described (16). For database searches by MS-Fit (University of California, San Francisco), the following parameters were used. Trypsin max missed cleavages = two, constant modification was carbamidomethyl (C), masses were monoisotopic, mass tolerance was 50 to 75 ppm, the instrument was MALDI-TOF/TOF, and the data format was PP M/Z intensity charge.

For DGCR14 complex purification, I generated a retroviral vector expressing DGCR14-Flag and transduced it into 68-41 cells. Cultured DGCR14-Flag-expressing 68-41 cells were treated for nuclear extract preparation. Nuclear extracts were then fractionated by glycerol density gradient centrifugation (10 to 40% glycerol in buffer D, 18,000 rpm, 4°C, 20 h). After Western blotting (see Fig. 4A), DGCR14-Flag-expressing fractions were collected and precipitated with anti-Flag M1 agarose affinity gel (Sigma) and then eluted with 100 μg ml^{-1} Flag peptide (Sigma) in buffer D.

Plasmid constructs. The full-length mouse RORγt cDNA expression vector and m*Il17a* promoter luciferase vector used were described previously (14). Deletion mutant variants of mouse RORγt were amplified by standard PCR techniques and cloned with the CMV-T7 vector. Full-length cDNAs for *DGCR14*, *RpS6ka1*, *RpS6ka2*, and *RpS6ka3* were amplified by standard PCR techniques and cloned with a Flag tag into pcDNA3 (Invitrogen). Retroviral vectors expressing *Dgcr14* cDNA were amplified by standard PCR techniques and cloned into e-MIGR1 by XhoI and EcoRI. Retroviral vectors of short hairpin RNAs (shRNAs) were synthesized oligonucleotides (see Table S3 in the supplemental material) that were amplified and cloned into vectors (Open Biosystems EAV4678 and EAV4679) according to the manufacturer's protocol (17). The mouse *Dgcr14* promoter (−1 to −2364) was amplified by standard PCR techniques and cloned into a luciferase reporter vector. The full-length *Baz1b* cDNA expression vector was a gift from S. Kato (Soma Central Hospital).

Primary T cell differentiation. $CD4^+$ $CD25^-$ $CD44^{low}$ $CD62L^{high}$ naive T cells from spleens and lymph nodes were enriched through negative selection with a magnetic cell-sorting system (MACS; Miltenyi Biotec, Bergisch Gladbach, Germany) with biotin-conjugated anti-CD8.2 (53-6.7), anti-B220/CD44 (RA3-6B2), anti-CD11b (M1/70), anti-CD11c (N418), anti-CD49b (Dx5) (all from eBioscience, San Diego, CA), and anti-TER119 (BD Biosciences) antibodies, as well as streptavidin-conjugated magnetic beads (Miltenyi Biotec). Cells were then flow cytometrically sorted with a BD FACSAria cell sorter (BD Biosciences). The purity of the sorted $CD4^+$ T cell populations was consistently >98%. T cells were maintained in a complete medium containing RPMI 1640 supplemented with 10% FBS, 50 U penicillin, 50 μg ml^{-1} streptomycin, 100 nM nonessential amino acids, 2 mM glutamine, and 0.05 mM 2-mercaptoethanol. The culture conditions for different T_H cell subsets were as follows: 1 μg ml^{-1} anti-CD-3ε and 1 μg ml^{-1} anti-CD-28 for T_H0 (neutral conditions); 1 μg ml^{-1} anti-CD-3ε, 1 μg ml^{-1} anti-CD-28, 1 μg ml^{-1} anti-IL-4, and 10 ng ml^{-1} IL-12 (Peprotech) for T_H1; 1 μg ml^{-1} anti-CD-3ε, 1 μg ml^{-1} anti-CD-28, 1 μg ml^{-1} anti-gamma interferon (anti-IFN-γ), and 1 ng ml^{-1} IL-4 (Peprotech) for T_H2; 1 μg ml^{-1} anti-CD-3ε, 1 μg ml^{-1} anti-CD-28, 1 μg ml^{-1} anti-IL-4, 1 μg ml^{-1} anti-IFN-γ, and 2 ng ml^{-1} TGF-β (Peprotech) for inducible T_{reg}; and 1 μg ml^{-1} anti-CD-3ε, 1 μg ml^{-1} anti-CD-28, 1 μg ml^{-1} anti-IL-4, 1 μg ml^{-1} anti-IFN-γ, 10 ng ml^{-1} IL-6 (Peprotech), and 2 ng ml^{-1} TGF-β for T_H17.

For transduction with retroviruses, the following procedure was utilized. Isolated naive $CD4^+$ T cells were cultured under the appropriate conditions for 29 h, and concentrated viruses were transduced with 1.6 ng ml^{-1} Polybrene and centrifuged at 3,000 rpm at 37°C for 1.5 h. The cells were incubated at 37°C in 5% CO_2 overnight, after which they were washed and cultured for 2 to 4 days under the condition designated.

Flow cytometric analysis. For intracellular cytokine staining, cells were stimulated for 4 h in complete medium with phorbol 12-myristate 13-acetate (50 ng ml^{-1}) and ionomycin (500 ng ml^{-1}) (both from Sigma-Aldrich) in the presence of 3 μg ml^{-1} brefeldin A (eBioscience). Surface staining was then performed in the presence of Fc-blocking antibodies (2.4G2), followed by intracellular staining with anti-IL-17A antibody (eBioscience) or anti-IFN-γ antibody (eBioscience) with the Fixation and Permeabilization kit (eBioscience) according to the manufacturer's instructions. Data were acquired on a BD FACSCanto and analyzed with FlowJo software (TreeStar, Ashland, OR).

ELISA. Supernatants were collected after the cell culture periods indicated and analyzed for IL-17A with an enzyme-linked immunosorbent assay (ELISA) kit (eBioscience) and for IL-4 and IFN-γ with ELISA kits (R&D) according to the manufacturers' instructions.

Antibodies, Western blotting, immunoprecipitation, and ChIP. For Western blotting and/or chromatin immunoprecipitation (ChIP) analysis, I used antibodies against RORγ (PP-H6437; Perseus Proteomics), ROR common (PP-H3925; Perseus Proteomics), DGCR14 (sc-86411; Santa Cruz), RSK2 (ab32133; Abcam), BAZ1B (ab50632; Abcam), RIP140 (sc-8997; Santa Cruz), Flag (F3165; Sigma-Aldrich), and H3K9Me3 (07-442; Millipore).

For immunoprecipitation of cells transfected with the plasmids indicated, 293T or 68-41 cells (about 5×10^7) were washed with ice-cold phosphate-buffered saline. Cells were collected and resuspended in 100 μl lysis buffer (20 mM Tris-HCl [pH 7.9], 1% NP-40, 1 mM EDTA, 150 mM NaCl, 2.5 mM $MgCl_2$, 5% glycerol, 5 mM DTT, 10 mg ml^{-1} aprotinin, 1 mM PMSF), incubated on ice for 30 min, and centrifuged for 30 min at 12,000 × *g*. The resultant supernatants were diluted 10-fold with lysis buffer without NP-40 and used as whole-cell extracts for immunoprecipitation with the antibodies indicated with protein G-Sepharose (GE Healthcare) or Dynabeads Protein G (Life Technologies). After separation by SDS-PAGE, proteins were transferred to a PVDF membrane and Western blotting was performed.

ChIP was performed according to the manufacturer's protocol (Millipore). Briefly, cells were fixed with 1% formaldehyde (Sigma) and chromatin was sheared by sonication to average lengths of 300 to 500 bp. Chromatin was immunoprecipitated with control IgG or specific antibodies overnight at 4°C and then incubated with protein A-agarose-salmon sperm DNA (Millipore) for an additional 2 h. After washing and elution, protein-DNA cross-links were disrupted by heating at 65°C overnight. Immunoprecipitated DNA was purified with QIAquick spin columns (Qiagen) and analyzed by quantitative PCR (qPCR) with the CFX96 Touch real-time PCR detection system with SYBR green (Bio-Rad). The relative quantitation value is expressed as $2^{-\Delta CT}$, where ΔC_T is the difference between the mean C_T value of triplicates of the sample and that of the input control. The sequences of the primers used are shown in Table S3 in the supplemental material.

RNA analysis. Total RNA was extracted with TRIzol (Invitrogen, Carlsbad, CA). First-strand cDNA was synthesized from total RNA with the SuperScript III synthesis system (Invitrogen) and random hexamer primers. The gene expression levels were analyzed by reverse transcription (RT)-qPCR with the CFX96 Touch real-time PCR detection system with SYBR green (Bio-Rad). The relative quantitation value is expressed as $2^{-\Delta CT}$, where ΔC_T is the difference between the mean C_T value of triplicates of the sample and that of the *Gapdh* control. The sequences of the primers used are shown in Table S3 in the supplemental material.

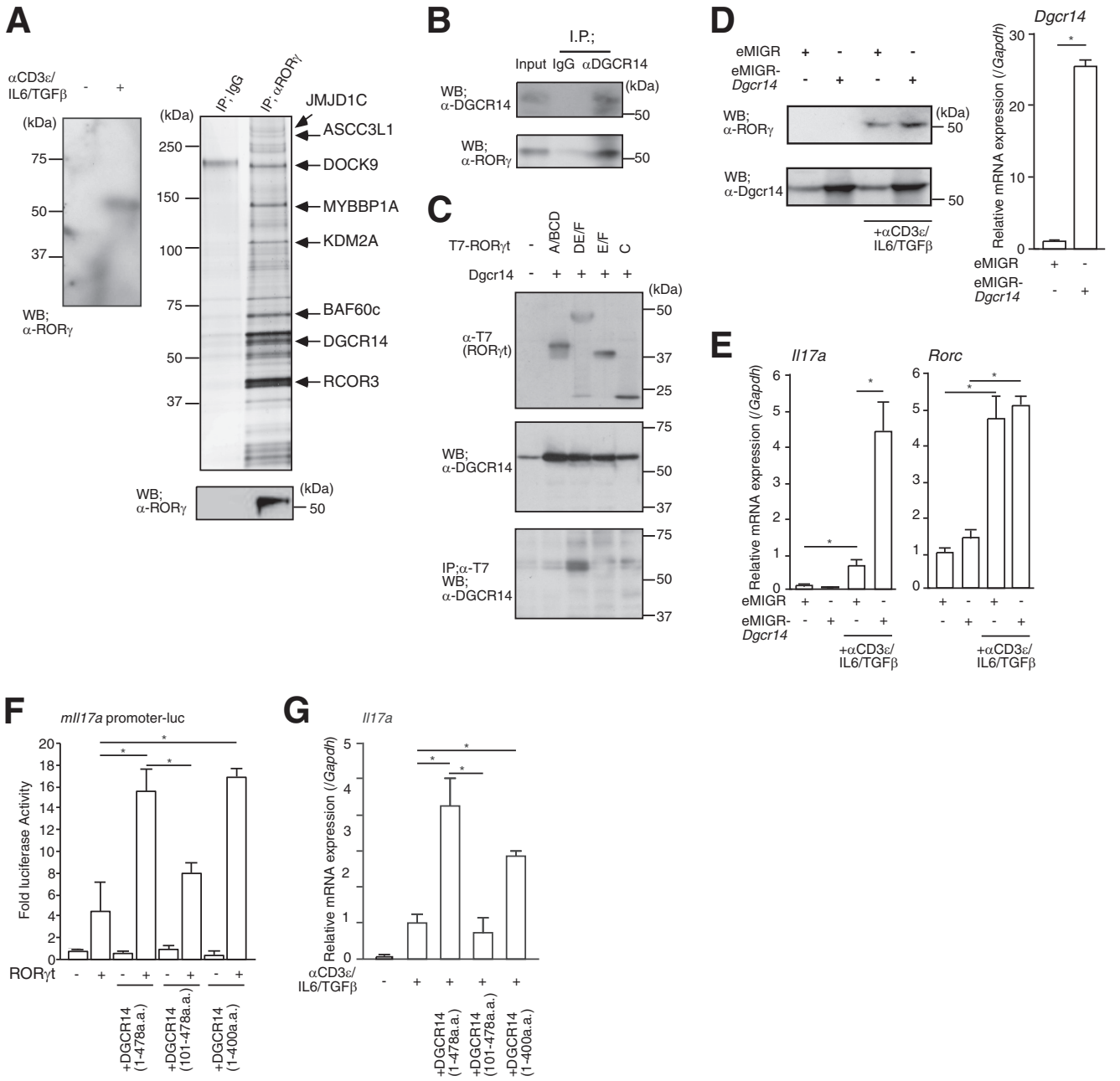

FIG 1 Identification of DGCR14 as a transcriptional coactivator of RORγ. (A) The left panel shows Western blotting for RORγ in 68-41 cells. After stimulation with or without anti-CD3ε antibody, IL-6, and TGF-β, nuclear extracts were prepared and Western blot (WB) assays were performed with the antibodies indicated. The right upper panel shows purification of RORγ-associated proteins from the 68-41 T cell hybridoma line. Large-scale cultures of 68-41 cells were stimulated with anti-CD3ε antibody, IL-6, and TGF-β for 8 h. Nuclear extracts were prepared and purified on anti-RORγ affinity columns and eluted with 0.1 M glycine, pH 3.0. Samples were separated by SDS-PAGE, silver stained, and identified by MALDI-TOF MS analysis (see Table S1 in the supplemental material). Eluted RORγ was detected by Western blotting with anti-RORγ antibody (right lower panel). IP, immunoprecipitation. (B) Immunoprecipitation assays with anti-DGCR14 antibody in 68-41 cells. After stimulation with anti-CD3ε antibody, IL-6, and TGF-β, cells were lysed and precipitated with rabbit IgG or anti-DGCR14 antibody. Western blot assays were performed with the antibodies indicated. (C) Immunoprecipitation assays with T7-tagged RORγt deletion mutant variants (A/BCD, DE/F, E/F, and C). After transfection with each expression vector, 293T cells were lysed and precipitated with anti-T7 antibody (MBL). Western blot assays were performed with the antibodies indicated. (D) The left panels show Western blotting for RORγ and DGCR14 in 68-41 cells with or without *Dgcr14* cDNA retroviruses and stimulation with anti-CD3ε antibody, IL-6, and TGF-β. After infection of 68-41 cells with each virus, virus-expressing green fluorescent protein (GFP)-positive cells were sorted with a FACSAria (BD) and cultured. After stimulation with anti-CD3ε antibody, IL-6, and TGF-β, cells were lysed and Western blotting was performed with the antibodies indicated. The right panel shows RT-qPCR analysis for *Dgcr14* mRNA in 68-41 cells transduced with *Dgcr14* cDNA. Each experiment was performed at least three times, and results are presented as means ± SD. *, $P < 0.05$. (E) RT-qPCR analyses for *Il17a* and *Rorc* mRNAs in 68-41 cells transduced with *Dgcr14* cDNA. After stimulation with or without anti-CD3ε antibody, IL-6, and TGF-β, RNA was extracted and RT-qPCR was performed. The mRNA levels of all genes were normalized to the level of *Gapdh* mRNA expression. Each experiment was performed at least three times, and results are presented as means ± SD. *, $P < 0.05$. (F) Luciferase reporter assays with *Dgcr14* deletion mutant variants and the m*Il17a* promoter-luciferase reporter vector. After the transduction of each *Dgcr14* deletion cDNA expression vector and RORγt expression vector, 68-41 cells were stimulated with anti-CD3ε antibody, IL-6, and TGF-β. The cells were then lysed and used in luciferase reporter assays. As an internal control, *o*-nitrophenyl-β-D-galactopyranoside (ONPG)-dependent β-gal activities were measured with a microplate reader. Each experiment was performed at least three times, and results are presented as means ± SD. *, $P < 0.05$. (G) RT-qPCR for assessment of *Il17a* mRNA in 68-41 cells as described for panel F. The mRNA levels of all genes were normalized to the level of *Gapdh* mRNA expression. Each experiment was performed at least three times, and results are presented as means ± SD. *, $P < 0.05$.

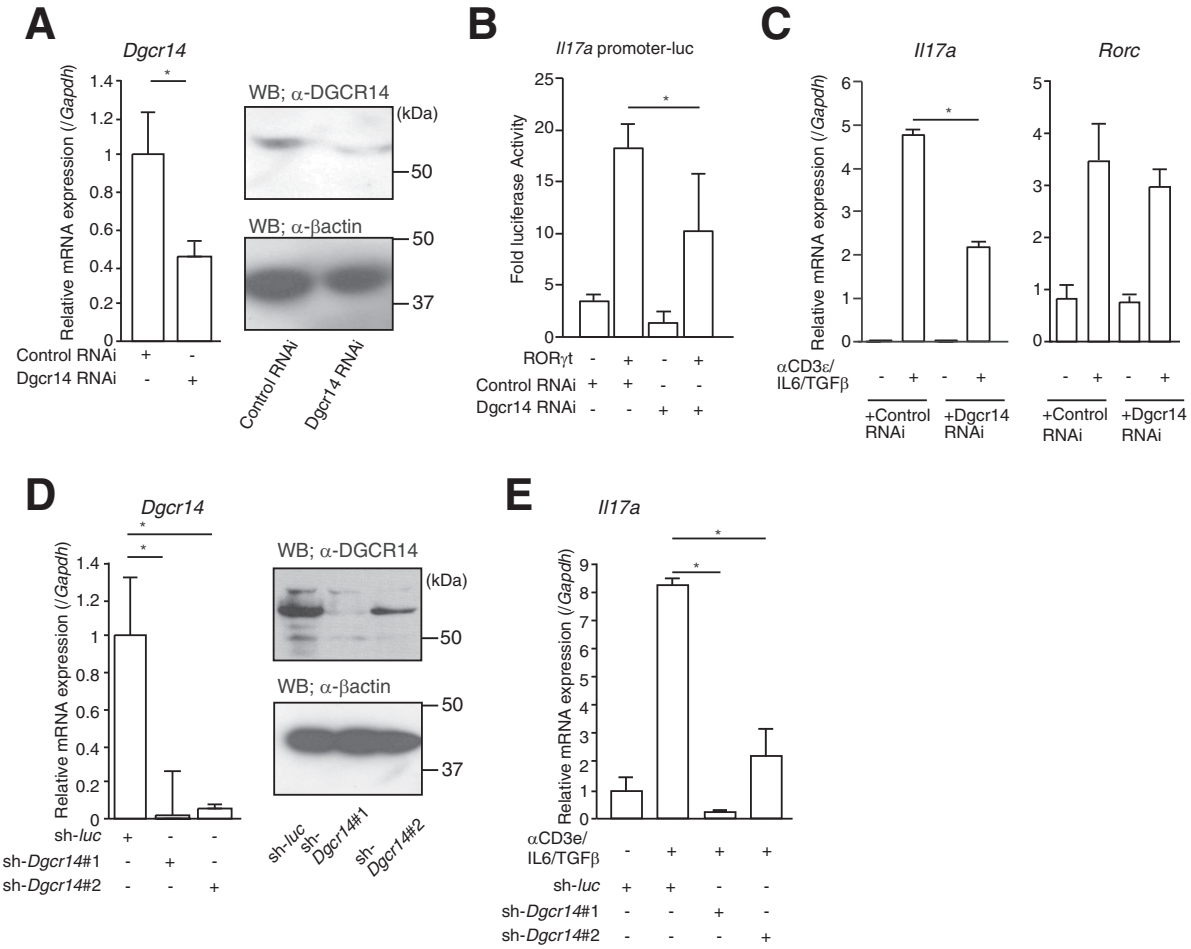

FIG 2 Knockdown of *Dgcr14* mRNA suppressed the function of RORγt. (A) The left panel shows RT-qPCR for assessment of *Dgcr14* in 68-41 cells transfected with control or *Dgcr14* RNAi-expressing vectors. The mRNA levels of all genes were normalized to the level of *Gapdh* mRNA expression. Each experiment was performed at least three times, and results are presented as means ± SD. *, $P < 0.05$. The right panels show Western blotting for DGCR14 proteins in 68-41 cells transfected with control or *Dgcr14* RNAi-expressing vectors. (B) Luciferase reporter assay of 68-41 cells. After transfection with *Dgcr14* RNAi expression vectors, an m*Il17a* promoter luciferase vector, a β-gal expression vector, and/or a RORγt expression vector, cells were cultured for 1 day. Cells were then harvested, and luciferase assays were performed. As an internal control, ONPG-dependent β-gal activities were measured with a microplate reader. Each experiment was performed at least three times, and results are presented as means ± SD. *, $P < 0.05$. (C) RT-qPCR analysis of *Dgcr14* RNAi-expressing 68-41 cells. After transfection with or without *Dgcr14* RNAi expression vectors, 68-41 cells were cultured with or without anti-CD3ε antibody, IL-6, and TGF-β. RNA was extracted and RT-qPCR was performed. The mRNA levels of all genes were normalized to the level of *Gapdh* mRNA expression. Each experiment was performed at least three times, and results are presented as means ± SD. *, $P < 0.05$. (D) The left panel shows RT-qPCR assessment for *Dgcr14* mRNA in 68-41 cells transduced with control (sh-*luc*)- or two *Dgcr14* shRNA-expressing retroviruses (sh-*Dgcr14*#1 and sh-*Dgcr14*#2). The mRNA levels of all genes were normalized to the level of *Gapdh* mRNA expression. After transduction with each virus, GFP-positive cells were isolated with a FACSAria (BD) and cultured. Among six shRNAs for *Dgcr14*, two shRNAs targeting *Dgcr14* reduced its mRNA levels. Each experiment was performed at least three times, and results are presented as means ± SD. *, $P < 0.05$. The right panels show Western blotting for DGCR14 in 68-41 cells transduced with control or *Dgcr14* shRNA-expressing retroviruses. Western blot assays were performed with the antibodies indicated. (E) RT-qPCR assessment of *Il17a* mRNA in 68-41 cells transduced with control or *Dgcr14* shRNA-expressing retroviruses. The mRNA levels of all genes were normalized to the level of *Gapdh* mRNA expression. Each experiment was performed at least three times, and results are presented as means ± SD. *, $P < 0.05$.

Luciferase reporter assays. Luciferase assays were performed as previously described (18). Briefly, cells at 40 to 50% confluence were transfected with the plasmids indicated with the Lipofectamine Plus reagent (Invitrogen) in 24-well plates. The total amount of DNA was adjusted by supplementation with the empty vector up to 1.0 μg well^{-1}. Luciferase activity was determined with the luciferase assay system (Promega). As a reference plasmid to normalize transfection efficiency, 10 ng well^{-1} of plasmid pCMV-βgal was cotransfected in all experiments and β-galactosidase (β-gal) assays were performed.

Statistical analysis. Data are presented as means ± the standard deviations (SD). Differences between groups were assessed by Student's paired two-tailed *t* test. *P* values of <0.05 were considered significant. All of the error bars shown represent standard deviations.

RESULTS

DGCR14 promoted T_H17 cell differentiation by coactivating RORγ/γt function. To purify RORγ-associated proteins, I used the 68-41 murine T cell hybridoma cell line (19), which upregulates RORγ protein and *Il17a* mRNA expression when treated with anti-CD3ε antibody, TGF-β, and IL-6 (17) (Fig. 1A, left panel). After preparing nuclear extracts according to classical methods (15), RORγ interactants were purified by using an anti-RORγ antibody column and subsequently identified by MALDI-TOF MS (Fig. 1A, right panels). I identified several known transcriptional coregulators (see Table S1 in the supplemental

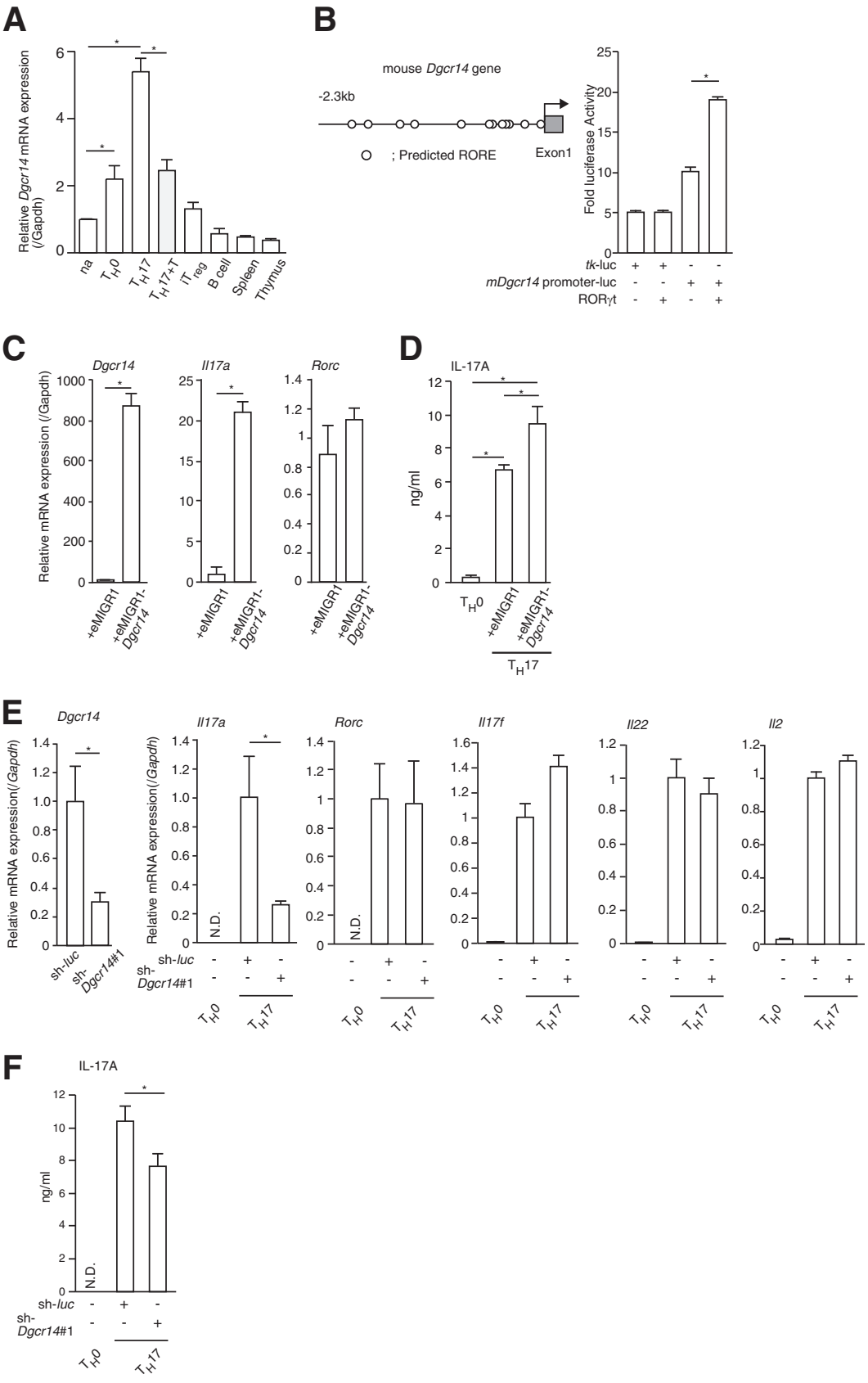
A
Relative Dgcr14 mRNA expression (/Gapdh)
na
TH0
TH17
TH17+T
iTreg
B cell
Spleen
Thymus
B
mouse Dgcr14 gene
-2.3kb
; Predicted RORE
Exon1
Fold luciferase Activity
tk-luc
mDgcr14 promoter-luc
RORγt
C
Dgcr14
Il17a
Rorc
Relative mRNA expression (/Gapdh)
+eMIGR1
+eMIGR1-Dgcr14
D
IL-17A
ng/ml
TH0
TH17
E
Dgcr14
Il17a
Rorc
Il17f
Il22
Il2
Relative mRNA expression(/Gapdh)
sh-luc
sh-Dgcr14#1
N.D.
F
IL-17A
ng/ml

material), including histone-modifying enzymes (JMJD1C and KDM2A), a subunit of the chromatin-remodeling complex (BAF60c) and other transcriptional coregulators (ASCC3L1, MYBBP, and RCOR3). Among the factors identified, I focused on the DGCR14/ES2 protein. *Dgcr14*/*Es2* is one of the genes deleted in DiGeorge or 22q11.2 deletion syndrome (20, 21), which is characterized by various defects of the heart, thymus, and parathyroid gland (22). DGCR14 is a nuclear protein with a coiled-coil domain (21) that is conserved in lower species, including *Drosophila melanogaster* (23), *Caenorhabditis elegans* (24), and yeast (25). Although recent studies showed that DGCR14/ES2 associates with other nuclear proteins (26) or the splicing complex (27), the role of DGCR14 in T lymphocytes is not fully understood. Endogenous DGCR14 protein associates with RORγ in 68-41 cells stimulated with anti-CD3ε antibody, IL-6, and TGF-β (Fig. 1B).

To better assess the role of DGCR14, I mapped the interaction domain between RORγt and DGCR14 by immunoprecipitation assay. RORγt consists of an activation function 1 (AF1) region (A/B), a C4-type Zn finger domain (a DNA binding region; C), a hinge region (D), and a ligand and coactivator binding site including AF2 (E/F). I generated four RORγt deletion mutant variants (A/BCD, amino acids [aa] 1 to 244; DE/F, aa 74 to 495; E/F, aa 245 to 495; C, aa 4 to 74) and found that the DE/F region of RORγt associated with DGCR14 (Fig. 1C). This region is conserved between RORγ and RORγt. I then established a stably expressed *Dgcr14* cDNA in 68-41 cells by transducing eMIGR-*Dgcr14* retroviruses (Fig. 1D) and examined mRNA levels of *Il17a* by RT-qPCR. As shown in Fig. 1E, Dgcr14 overexpression strongly induced levels of *Il17a* but not *Rorc* mRNA.

In addition, luciferase reporter assays using the murine *Il17a* (m*Il17a*) promoter in 68-41 cells showed that the N-terminal domain of DGCR14 was required for DGCR14-dependent coactivation of RORγt function (Fig. 1F). Overexpression of these mutant DGCR14 proteins showed the significance of the N-terminal domain (aa 1 to 100) of DGCR14 in *Il17a* mRNA expression (Fig. 1G), although this domain does not show any similarities to known transcriptional coactivation domains.

Dgcr14 knockdown suppressed the transcriptional activity of RORγ/γt. To investigate the effect of Dgcr14 on *Il17a* mRNA expression, I transfected vectors expressing interfering RNA (RNAi) for *Dgcr14* into 68-41 cells and conducted luciferase reporter assays. As expected, *Dgcr14* knockdown inhibited the transcriptional activity of RORγt on the *mIl17a* promoter (Fig. 2A and B). Moreover, endogenous *Il17a* mRNA levels were also reduced by *Dgcr14* RNAi-expressing 68-41 cells stimulated with anti-CD3ε antibody, IL-6, and TGF-β (Fig. 2C). I then transduced a retrovirus vector expressing shRNA for *Dgcr14* mRNA into 68-41 cells. I tested several shRNAs for *Dgcr14* mRNA and found one that effectively downregulated *Dgcr14* mRNA expression (Fig. 2D; see Table S3 in the supplemental material). This shRNA (sh-*Dgcr14*#1) also reduced mRNA levels of *Il17a* in 68-41 cells stimulated with anti-CD3ε antibody, IL-6, and TGF-β (Fig. 2E). These results clearly showed the role of DGCR14 as a transcriptional coactivator in T-lymphocyte-related cells.

DGCR14 regulated *Il17a* mRNA expression in primary T_H17 cells. My results showed that DGCR14 coactivated the transcriptional activity of RORγt in 68-41 cells, but the role of DGCR14 in primary cultured T_H17 cells remained unclear. *Dgcr14* mRNA expression levels were higher in cultured primary T_H17 cells than in naive T and T_H0 cells (Fig. 3A). Interestingly, T0901317, a partial agonist of RORγ, reduced mRNA levels of *Dgcr14* (Fig. 3A). This result raises the possibility that *Dgcr14* mRNA expression was regulated by RORγ/γt. The mouse *Dgcr14* promoter region contains several ROREs (5′-AGGTCA-3′), and I cloned the *mDgcr14* promoter region and subjected it to luciferase reporter assays. As shown in Fig. 3B, RORγt overexpression modestly induced *Dgcr14* gene promoter activities. These results show that RORγt partially regulates Dgcr14 mRNA expression.

I then transduced retroviruses expressing *Dgcr14* cDNA into primary cultured T_H17 cells. I found that *Il17a* expression was consistently enhanced but *Rorc* mRNA levels were unchanged (Fig. 3C and D). As expected, *Dgcr14* shRNA reduced *Il17a* mRNA and protein expression in cultured primary T_H17 cells (Fig. 3E and F). These results indicated that DGCR14 mRNA is induced during $CD4^+$ helper T cell differentiation, at least in part, by regulating the transcriptional activation of RORγ/γt.

RSK2 and BAZ1B coactivated the transcriptional activity of RORγ/γt. In general, transcriptional coregulator function is achieved by forming a complex that includes a chromatin-remodeling factor and histone-modifying enzymes (28). DGCR14 protein does not have known domains for histone-modifying enzyme activity or chromatin-remodeling activity. In addition, I found that DGCR14 was associated with other transcriptional factors and regulated their functions (data not shown). Therefore, I hy-

FIG 3 DGCR14 induced IL17A expression in primary cultured T_H17 cells. (A) RT-qPCR analysis of *Dgcr14* mRNA in $CD4^+$ helper T cells, B cells, thymus cells, and spleen cells. Isolated naive T cells (na) were cultured under T_H0, iTreg, or T_H17 conditions. T_H17 cells treated with 10 μM T0901713 (T_H17+T) reduced *Dgcr14* mRNA expression. B cells were isolated with anti-CD19 microbeads with a MACS (Miltenyi Biotec). After RNAs were extracted and cDNAs were synthesized, real-time PCR was performed. The mRNA levels of all genes were normalized to the level of *Gapdh* mRNA expression. Each experiment was performed at least three times, and results are presented as means ± SD. *, $P < 0.05$. (B) Luciferase reporter assay of 293T cells. The mouse *Dgcr14* gene promoter regions are shown in the left panel. After transfection with a tk-luc or m*Dgcr14* promoter-tk-luc reporter vector (m*Dgcr14* promoter-luc), a β-gal expression vector, and/or an RORγt expression vector, cells were cultured for 1 day. Cells were then harvested, and luciferase assays were performed. As an internal control, ONPG-dependent β-gal activities were measured with a microplate reader. Each experiment was performed at least three times, and results are presented as means ± SD. *, $P < 0.05$. (C) RT-qPCR analysis of *Dgcr14*-overexpressing primary cultured $CD4^+$ T cells under T_H17 conditions. eMIGR1-control or eMIGR1-*Dgcr14* retroviruses were transduced into primary cultured T_H17 cells (anti-CD3ε, -CD28, -IFN-γ and -IL-4 antibodies; 10 ng ml^{-1} IL-6; and 1 ng ml^{-1} TGF-β). GFP-expressing cells were sorted with a FACSAria (BD), and RT-qPCR was performed. The mRNA levels of all genes were normalized to the level of *Gapdh* mRNA expression. Each experiment was performed at least three times, and results are presented as means ± SD. *, $P < 0.05$. (D) ELISA of mIL-17A in T_H0, control, and *Dgcr14*-overexpressing primary T_H17 cells. After cultivation under the conditions indicated, supernatants were collected and analyzed. Each experiment was performed at least three times, and results are presented as means ± SD. *, $P < 0.05$. (E) RT-qPCR analysis of primary cultured T_H17 cells transduced with control (sh-*luc*)- or sh-*Dgcr14*#1-expressing retroviruses. After transduction with each virus, GFP-positive cells were isolated with a FACS Aria (BD) and RT-qPCR was performed. The mRNA levels of all genes were normalized to the level of *Gapdh* mRNA expression. Each experiment was performed at least three times, and results are presented as means ± SD. *, $P < 0.05$. (F) ELISA for IL-17A protein in primary cultured T_H0 cells and T_H17 cells transduced with control (sh-*luc*)- or sh-*Dgcr14*#1-expressing retroviruses. Each experiment was performed at least three times, and results are presented as means ± SD. *, $P < 0.05$. N.D., not determined.

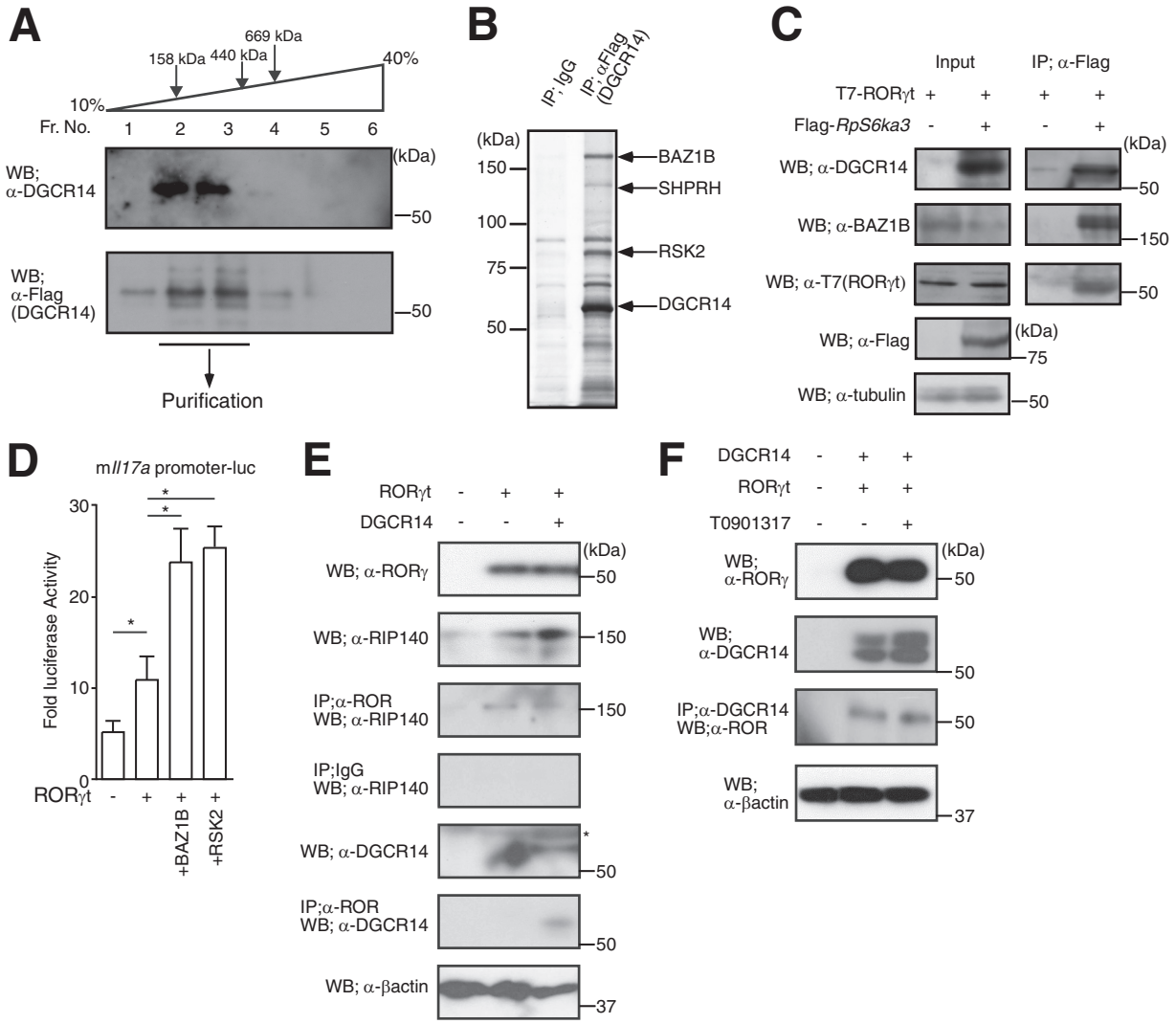

FIG 4 DGCR14 was associated with BAZ1B and RSK2. (A) Western blotting of DGCR14 in 68-41 cells. For biochemical purification, nuclear extracts of DGCR14-Flag-expressing 68-41 cells were prepared. After fractionation by glycerol density gradient centrifugation, each fraction was analyzed by Western blotting with the antibodies indicated. Fractions (Fr. No.) 2 and 3 were subjected to further purification with anti-Flag M1 agarose affinity gel. (B) Biochemical purification of DGCR14-associated proteins. After the establishment of DGCR14-Flag-expressing 68-41 cells, nuclear extracts were prepared and purified with anti-Flag M1 agarose affinity gel. Samples were eluted by Flag peptide and subjected to SDS-PAGE and silver stained, and proteins were identified by MALDI-TOF MS (see Table S2 in the supplemental material). (C) Immunoprecipitation assays of DGCR14 and RSK2 in 293T cells. After transfection with T7-RORγt and/or Flag-RSK2 expression vectors, cells were incubated for 1 day and lysed. Samples were then immunoprecipitated with anti-Flag M1 agarose affinity gel and examined by Western blotting with the antibodies indicated. (D) Luciferase reporter assay of the m*Il17a* promoter in 293T cells. After transfection with a β-gal expression vector, a m*Il17a* promoter luciferase vector, and/or expression vectors for *RORγt*, *Rps6ka3*, or *Baz1b*, 293T cells were cultured for 36 h and collected and luciferase assays were performed. As an internal control, ONPG-dependent β-gal activities were measured with a microplate reader. Each experiment was performed at least three times, and results are presented as means ± SD. *, $P < 0.05$. (E) Immunoprecipitation assays of DGCR14, RORγt, and RIP140 in 293T cells. After transfection with expression vectors for *RORγt* and/or *Dgcr14*, cells were incubated for 1 day and lysed. Samples were then immunoprecipitated with anti-ROR common and examined by Western blotting with the antibodies indicated. The asterisk indicates a nonspecific band. (F) Immunoprecipitation assays of DGCR14 and RORγt in 293T cells with or without T0901317. After transfection with expression vectors for *RORγt* and/or *Dgcr14*, cells were incubated for 1 day with or without 10 μM T0901317 and lysed. Samples were then immunoprecipitated with anti-DGCR14 and examined by Western blotting with the antibodies indicated.

pothesized that DGCR14 regulated the transcriptional activity of several transcriptional factors by associating with other proteins. To characterize the function of DGCR14 in transcriptional regulation, I further enriched DGCR14-associated proteins by biochemical purification (Fig. 4A and B). I was unable to generate 68-41 cells expressing DGCR14 protein tagged with Flag peptide in the N-terminal region. Thus, I generated a retroviral vector expressing DGCR14 protein Flag tagged in the C-terminal region and established 68-41 cells stably expressing DGCR14-Flag. As shown in Fig. 4A, a nuclear extract was fractionated by glycerol gradient ultracentrifuge to enrich the DGCR14-expressing fraction (fractions 2 and 3, Fig. 4A). After elution with Flag peptide, BAZ1B, SHPRH, and RSK2 were identified as DGCR14-associated proteins (see Table S2 in the supplemental material). BAZ1B is a subunit of ATP-dependent chromatin remodelers and plays various roles in the nucleus, including participation in transcrip-

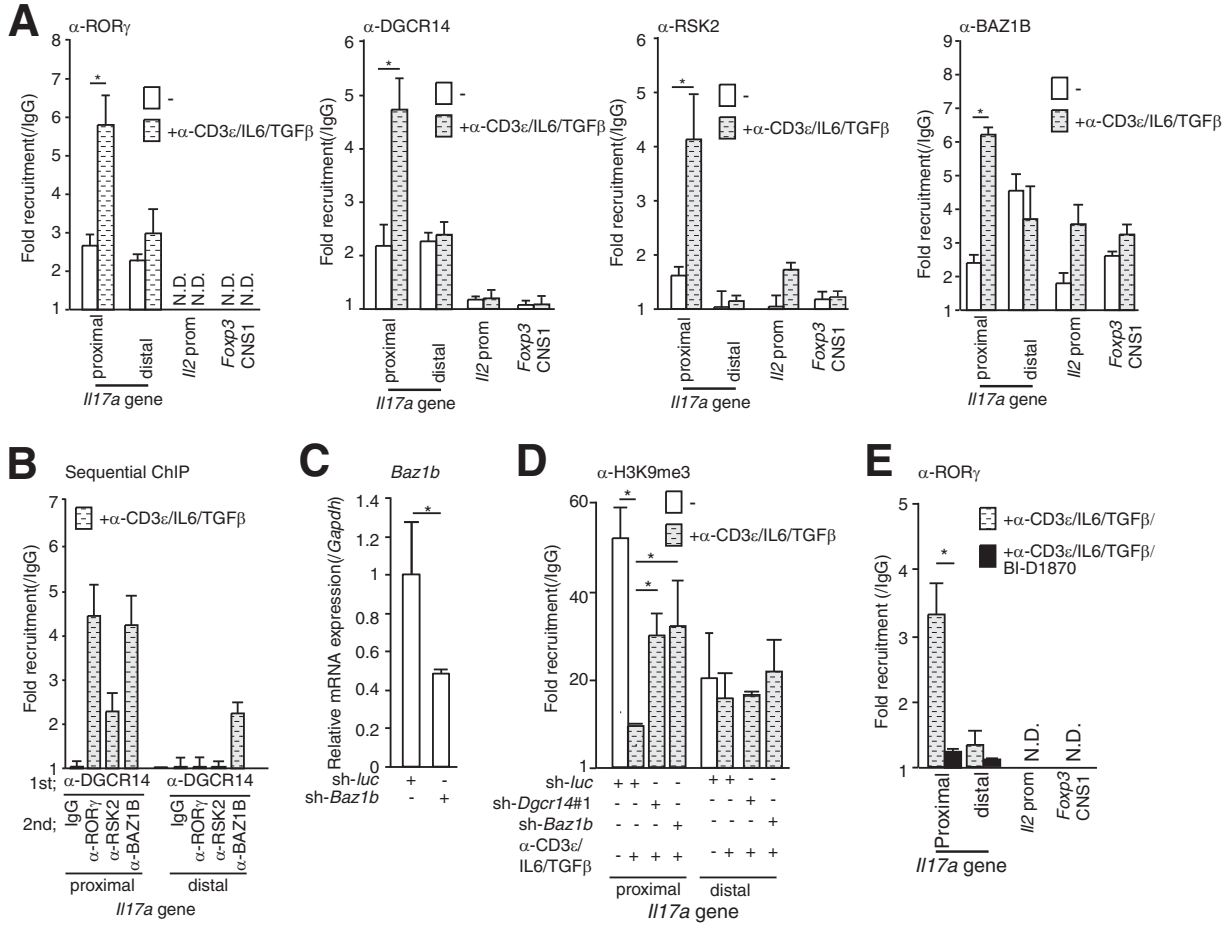

FIG 5 ChIP analysis of the m*Il17a* promoter. (A) ChIP analysis of the *Il17a* promoter with anti-RORγ, anti-RSK2, anti-BAZ1B, and anti-DGCR14 antibodies in 68-41 cells. After cultivation of cells that were treated with or without anti-CD3ε antibody, IL-6, and TGF-β, cells were lysed and ChIP analyses were performed with the antibodies indicated. qPCR was performed with the primers indicated (see Table S3 in the supplemental material). (B) Sequential ChIP analysis of the m*Il17a* promoter in 68-41 cells treated with anti-CD3ε antibody, IL-6, and TGF-β. After immunoprecipitation with anti-DGCR14 antibodies, proteins were eluted with 10 mM DTT, ChIP analysis was conducted with the antibodies indicated, and qPCR was performed. The *Il2* promoter and *Foxp3 CNS1* were also examined, but a signal was not detected (data not shown). (C) RT-qPCR analysis of *Baz1b* in 68-41 cells transduced with the control (sh-*luc*)- or *Baz1b* shRNA (sh-*Baz1b*)-expressing retroviruses used in panel D. After transduction with each virus, GFP-positive cells were isolated with a FACS Aria (BD) and cultured. (D) ChIP analysis of the m*Il17a* promoter in sh-*luc*-, sh-*Dgcr14*#1-, or sh-*Baz1b*-expressing 68-41 cells. After cultivation with or without anti-CD3ε antibody, IL-6, and TGF-β, cells were lysed and ChIP analysis was performed with the anti-histoneH3K9Me3 antibody. A quantitative PCR assay was then performed with each primer. (E) ChIP analysis of the m*Il17a* promoter in 68-41 cells treated with anti-CD3ε antibody, IL-6, and TGF-β with or without BI-D1870. Cells were lysed, and ChIP analysis was performed with anti-RORγ antibody. Each experiment was performed at least three times, and results are presented as means ± SD. *, $P < 0.05$. N.D., not determined.

tion (29) and DNA damage repair (30). SHPRH is an E3 ubiquitin ligase involved in DNA repair (31). RSK2 consists of a group of serine/threonine kinases that are constituents of the AGC subfamily in the human kinome (32). RSK isoforms play an important role in the mitogen-activated protein kinase signaling cascade. RSK2 regulates ligand-inducible estrogen receptor activity by phosphorylation (33).

Immunoprecipitation assays showed that RSK2 associated with DGCR14, RORγt, and BAZ1 (Fig. 4C) and RSK2 and BAZ1B coactivated the transcriptional activities of RORγt on the m*Il17a* promoter (Fig. 4D). Furthermore, DGCR14 overexpression did not interfere with the interaction between RORγt and RIP140 (34) (Fig. 4E), and T0901317 did not suppress the association of RORγt and DGCR14 (Fig. 4F). These results showed that DGCR14 regulated the transcriptional activity of RORγt through RSK2/BAZ1B in an AF2-independent manner.

DGCR14, RSK2, and BAZ1B were bound to the *Il17a* promoter. The *Il17a* promoter contains binding elements for ROR and other transcriptional factors, including IRF4 (35), RUNX1 (36), NFATc (37), Foxp3 (14), and STAT3 (38). I performed ChIP analyses with anti-DGCR14 antibody on the *Il17a* gene (proximal, −179 to −72; distal, −9818 to −9670), the *Il2* promoter, and the conserved noncoding DNA sequence 1 (CNS1) region of the *Foxp3* locus (18). ChIP analysis of 68-41 cells treated with or without anti-CD3ε antibody, IL-6, and TGF-β showed that DGCR14, BAZ1B, and RSK2 were recruited to the *Il17a* promoter region in a manner dependent on anti-CD3ε antibody, IL-6, and TGF-β (Fig. 5A). I then performed sequential ChIP analyses of the *Il17a* and *Il2* promoters and *Foxp3* CNS1 in 68-41 cells stimulated with anti-CD3ε antibody, IL-6, and TGF-β. I first performed ChIP analysis with anti-DGCR14 antibody and then performed re-ChIP analysis with IgG and anti-RORγ, -RSK2, and -BAZ1B an-

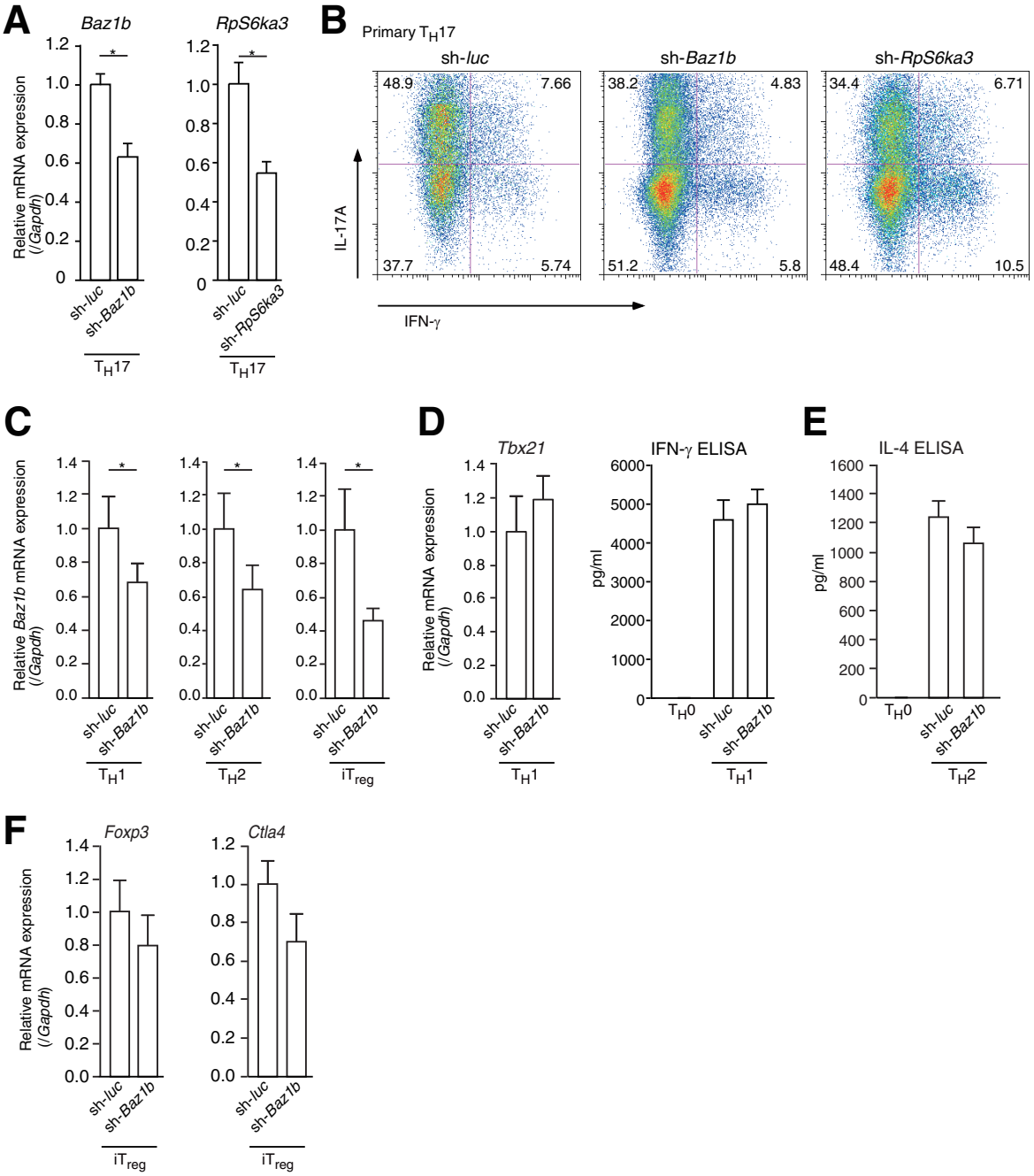

FIG 6 shRNA for *RpS6ka3* or *Baz1b* reduced T_H17 cell differentiation. (A) RT-qPCR analysis of *Rps6a3* and *Baz1b* mRNA expression in primary cultured T_H17 cells expressing shRNAs for *Rps6a3* (sh-*RpS6ka3*) or *Baz1b* (sh-*Baz1b*). The mRNA levels of all genes were normalized to the level of *Gapdh* mRNA expression. Each experiment was performed at least three times, and results are presented as means ± SD. *, $P < 0.05$. (B) Effect of *Baz1b* or *Rps6ka3* shRNA on T_H17 differentiation. After transduction with control (sh-*luc*), *Baz1b* shRNA (sh-*Baz1b*), or *Rps6ka3* shRNA (sh-*Rps6ka3*) retrovirus, primary $CD4^+$ T cells were cultured under T_H17 conditions (anti-CD3ε, anti-CD28, anti-IFN-γ, and anti-IL-4 antibodies; 10 ng ml^{-1} IL-6; and 1 ng ml^{-1} TGF-β) for 4 days. Cells were then analyzed by flow cytometry. (C) RT-qPCR analysis of *Baz1b* mRNA expression in primary cultured T_H1, T_H2, and iT_{reg} cells expressing shRNA for *Baz1b* (sh-*Baz1b*). mRNA levels of *Baz1a* were normalized to the level of *Gapdh* mRNA expression. Each experiment was performed at least three times, and results are presented as means ± SD. *, $P < 0.05$. (D to F) RT-qPCR analysis of mRNA expression and ELISA for IFN-γ and IL-4 in primary cultured T_H1, T_H2, and iT_{reg} cells expressing shRNA for *Baz1b* (sh-*Baz1b*). The mRNA level of each gene was normalized to the level of *Gapdh* mRNA expression. Each experiment was performed at least three times, and results are presented as means ± SD. *, $P < 0.05$.

tibodies. As shown in Fig. 5B, DGCR14 was associated with RORγ, BAZ1B, and RSK2 in the m*Il17a* promoter region. Moreover, DGCR14 was not recruited to the m*Il2* promoter or the *Foxp3* CNS1 region but BAZ1B was bound to both regions. These results showed that DGCR14 regulated transcriptional activation by associating with RSK2 and BAZ1B as a transcriptional coactivator of RORγ but BAZ1B has distinct functions in the expression of other genes.

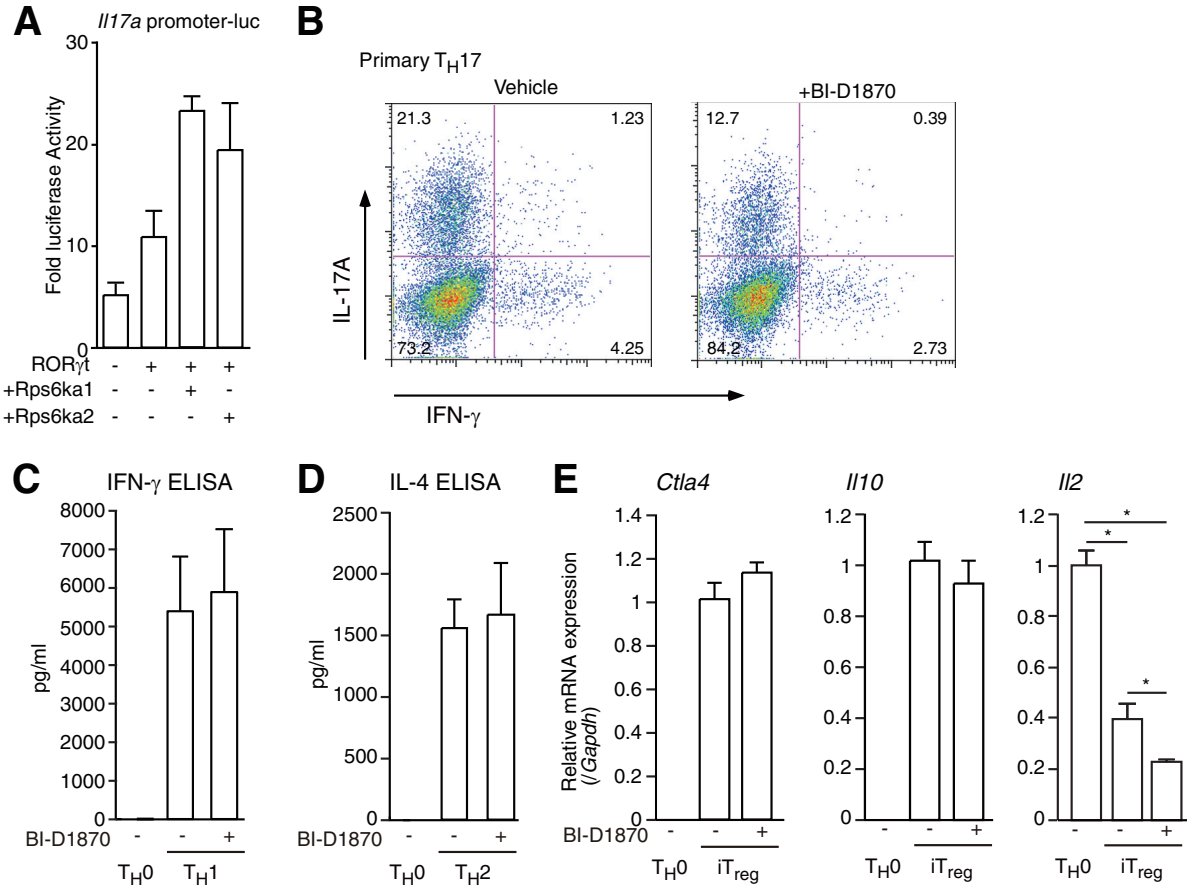

FIG 7 Effect of BI-D1870 on T_H17, T_H1, T_H2, and iT_{reg} differentiation. (A) Luciferase reporter assays of the m*Il17a* promoter in 68-41 cells. After transfection with a β-gal expression vector, an m*Il17a* promoter luciferase vector, and/or an expression vector for *RORγt*, *Rps6ka1*, or *Rps6ka2*, 68-41 cells were cultured for 36 h and collected and luciferase assays were performed. As an internal control, ONPG-dependent β-gal activities were measured with a microplate reader. Each experiment was performed at least three times, and results are presented as means ± SD. *, $P < 0.05$. (B) Flow cytometric analysis of primary cultured $CD4^+$ T cells under T_H17 conditions (anti-CD3ε, -CD28, -IFN-γ, and -IL-4 antibodies; 10 ng ml^{-1} IL-6; and 1 ng ml^{-1} TGF-β) with or without 10 μM BI-D1870 for 4 days. The cells were collected, and flow cytometric analysis was performed. (C) ELISA of IFN-γ protein in primary cultured T_H0 cells and T_H1 cells treated with or without BI-D1870. Each experiment was performed at least three times, and results are presented as means ± SD. *, $P < 0.05$. (D) ELISA of IL-4 protein in primary cultured T_H0 cells and T_H2 cells treated with or without BI-D1870. Each experiment was performed at least three times, and results are presented as means ± SD. *, $P < 0.05$. (E) Real-time RT-PCR analysis of iT_{reg} cells treated with or without 10 μM BI-D1870. After the isolation of RNAs from each tissue type, RT-qPCRs were performed. The mRNA levels of all genes were normalized to the level of *Gapdh* mRNA expression. Each experiment was performed at least three times, and results are presented as means ± SD. *, $P < 0.05$.

I next investigated whether shRNA for *Baz1b* (Fig. 5C) or *Dgcr14* affected the recruitment of a transcriptionally suppressive histone mark (histone H3K9me3) in the m*Il17a* promoter. As shown in Fig. 5D, both shRNAs increased histone H3K9me3 levels in the m*Il17a* promoter region in 68-41 cells stimulated with anti-CD3ε antibody, IL-6, and TGF-β. I then performed ChIP analysis of the *Il17a* promoter in 68-41 cells with an RSK inhibitor (BI-D1870). As shown in Fig. 5E, the pan-RSK inhibitor BI-D1870 reduced the recruitment of RORγ to the m*Il17a* promoter. These results showed that RSK activity and BAZ1B affected the recruitment of RORγ to the m*Il17a* promoter.

BAZ1B and RSK2 regulated *Il17a* mRNA expression in primary T_H17 cells. My results showed that RSK2 and BAZ1B were recruited to the m*Il17a* promoter and coactivated the function of RORγ/γt. *In vivo*, RSK2-deficient mice have reduced *Il2* mRNA expression in $CD4^+$ T cells (39) and *Baz1b* mutant mice have craniofacial features reminiscent of Williams syndrome (40). However, the role of RSK2 and BAZ1B in cultured primary T_H17 cells remains unclear.

I transduced *Baz1b* or *Rsk2* (*RpS6a3*) shRNA into primary T_H17 cells (Fig. 6A) and conducted flow cytometric analysis. Both of the shRNAs reduced IL17A protein levels in T_H17 cells (IFN-γ^- IL-$17A^+$ sh-*luc* T_H17 cells, 48.9%; sh-*Baz1b* T_H17 cells, 38.2%; sh-*RpS6a3* T_H17 cells, 34.4%) (Fig. 6B). Furthermore, I transduced *Baz1b* shRNA-expressing retroviruses into primary T_H1, T_H2, and iT_{reg} cells and performed RT-qPCR and ELISA (Fig. 6C to F). As shown in Fig. 6D to F, cell differentiation was not affected by *Baz1b* knockdown. These results showed that RSK2 and BAZ1B mainly promoted T_H17 cell differentiation.

RSK inhibitor BI-D1870 suppressed T_H17 differentiation. I identified DGCR14 as a transcriptional coactivator of RORγ/γt in T cells through BAZ1B/RSK2. I also used a pan-RSK inhibitor (BI-D1870 [41]) to investigate the effect of RSKs in helper T cell differentiation. The reason for using the pan-RSK inhibitor was

that RSK1 (*Rps6ka1*) and RSK3 (*Rps6ka2*) also coactivated the RORγt function on the *Il17a* promoter (Fig. 7A). First, I treated cells with BI-D1870 during T_H17 cell differentiation and found that BI-D1870 reduced the number of T_H17 cells (Fig. 7B) but did not change cell proliferation (Fig. 7C). I then treated primary T_H1, T_H2, and iT_{reg} cells with BI-D1870 and performed RT-qPCR and ELISA. As shown in Fig. 7C and D, BI-D1870 did not affect IFN-γ (T_H1) or IL-4 (T_H2) expression. For iT_{reg} cells, BI-D1870 reduced *Il2* expression but did not regulate *Il10* and *Ctla4* mRNA levels. These results showed that RSKs affected T_H17 differentiation.

DISCUSSION

In this study, I purified RORγ-associated proteins from T-lymphocyte-related cells. The cofactors identified, including histone-modifying enzymes and chromatin-remodeling factors, should be investigated further. Among them, I first characterized the role of DGCR14 as a transcriptional coregulator through RSK2 and BAZ1B. My findings revealed that BAZ1B plays pivotal roles in the recruitment and transactivation of RORγ/γt. I could not elucidate the precise molecular mechanism of DGCR14-dependent transcriptional activation. Deletion analysis of DGCR14 revealed that its N-terminal domain is critical for the coactivation of RORγt function. Thus, this N-terminal domain of DGCR14 might regulate the transcriptional activity. RORγ associates with many known transcriptional coactivators (2), and recent studies identified HSP90 and RIP140 as RORγ interactants in HepG2 hepatocarcinoma cells (34). These factors might regulate RORγt transcriptional activities synergistically with DGCR14, RSK2, and BAZ1B in T_H17 cells.

My study was unable to identify RSK2 phosphorylation sites associated with transcriptional activity. RSK phosphorylates R/KXRXXS/T or RRXS/T motifs (32). RSK phosphorylation sites in DGCR14 and BAZ1B have been conserved among species (DGCR14 [Thr382] and BAZ1B [Ser1240] in mice), but this is not the case for RORγ/γt. However, I could not determine the RSK2-dependent phosphorylation site affecting the transcriptional activity of RORγt (data not shown). The effects of an RSK2 inhibitor imply that RSK2 has a role in T_H17 cell differentiation, and further experiments are required to clarify this point.

Dgcr14 mRNA is expressed in many tissues, and DGCR14 protein regulates the transcriptional activity of other transcriptional factors such as PPARγ and c-Fos (data not shown). Thus, the function of Dgcr14 is expected in other tissues. The generation of knockout mice is required for further analysis.

In summary, I found novel RSK2- and BAZ1B-mediated transcriptional activation by DGCR14. These results provide key information for new approaches to autoimmune disease therapeutics. The combined use of RSK inhibitors and other autoimmune disease drugs such as RORγ/γt inverse agonists should effectively inhibit the development of autoimmune disease.

ACKNOWLEDGMENTS

I thank A. Yoshimura, M. Makishima, and S. Nakagawa for critical discussions. I particularly thank A. Yoshimura, who assisted me in this project. I also thank Y. Yogiashi, R. Tanikawa, and S. Fujiyama-Nakamura for helping with protein purification and proteomics. I thank R. Nakagawa, T. Shichita, and all laboratory members for useful discussions.

This work was supported by a grant-in-aid for Basic Research on Priority Areas (Dynamics of Extracellular Environments and Immunological Self), a grant-in-aid for Young Scientists (B; 23791662), a grant-in-aid for Scientific Research (C; 25462382), the Cell Science Research Foundation, the Kanae Foundation for the Promotion of Medical Science, and the Mochida Memorial Foundation.

REFERENCES

1. **Medvedev A, Yan ZH, Hirose T, Giguere V, Jetten AM.** 1996. Cloning of a cDNA encoding the murine orphan receptor RZR/ROR gamma and characterization of its response element. Gene **181:**199–206. http://dx.doi.org/10.1016/S0378-1119(96)00504-5.
2. **Jetten AM.** 2009. Retinoid-related orphan receptors (RORs): critical roles in development, immunity, circadian rhythm, and cellular metabolism. Nucl Recept Signal **7:**e003. http://dx.doi.org/10.1621/nrs.07003.
3. **Takeda Y, Kang HS, Freudenberg J, DeGraff LM, Jothi R, Jetten AM.** 2014. Retinoic acid-related orphan receptor gamma (RORgamma): a novel participant in the diurnal regulation of hepatic gluconeogenesis and insulin sensitivity. PLoS Genet **10:**e1004331. http://dx.doi.org/10.1371/journal.pgen.1004331.
4. **Kurebayashi S, Ueda E, Sakaue M, Patel DD, Medvedev A, Zhang F, Jetten AM.** 2000. Retinoid-related orphan receptor gamma (RORgamma) is essential for lymphoid organogenesis and controls apoptosis during thymopoiesis. Proc Natl Acad Sci U S A **97:**10132–10137. http://dx.doi.org/10.1073/pnas.97.18.10132.
5. **Ivanov II, McKenzie BS, Zhou L, Tadokoro CE, Lepelley A, Lafaille JJ, Cua DJ, Littman DR.** 2006. The orphan nuclear receptor RORgammat directs the differentiation program of proinflammatory IL-17$^+$ T helper cells. Cell **126:**1121–1133. http://dx.doi.org/10.1016/j.cell.2006.07.035.
6. **Kumar N, Lyda B, Chang MR, Lauer JL, Solt LA, Burris TP, Kamenecka TM, Griffin PR.** 2012. Identification of SR2211: a potent synthetic RORgamma-selective modulator. ACS Chem Biol **7:**672–677. http://dx.doi.org/10.1021/cb200496y.
7. **Solt LA, Kumar N, Nuhant P, Wang Y, Lauer JL, Liu J, Istrate MA, Kamenecka TM, Roush WR, Vidovic D, Schurer SC, Xu J, Wagoner G, Drew PD, Griffin PR, Burris TP.** 2011. Suppression of T_H17 differentiation and autoimmunity by a synthetic ROR ligand. Nature **472:**491–494. http://dx.doi.org/10.1038/nature10075.
8. **Wang Y, Kumar N, Nuhant P, Cameron MD, Istrate MA, Roush WR, Griffin PR, Burris TP.** 2010. Identification of SR1078, a synthetic agonist for the orphan nuclear receptors RORalpha and RORgamma. ACS Chem Biol **5:**1029–1034. http://dx.doi.org/10.1021/cb100223d.
9. **Kumar N, Solt LA, Conkright JJ, Wang Y, Istrate MA, Busby SA, Garcia-Ordonez RD, Burris TP, Griffin PR.** 2010. The benzenesulfoamide T0901317 [*N*-(2,2,2-trifluoroethyl)-*N*-[4-[2,2,2-trifluoro-1-hydroxy-1-(trifluoromethyl)ethyl]phenyl]-benzenesulfonamide] is a novel retinoic acid receptor-related orphan receptor-alpha/gamma inverse agonist. Mol Pharmacol **77:**228–236. http://dx.doi.org/10.1124/mol.109.060905.
10. **Stavreva DA, Varticovski L, Hager GL.** 2012. Complex dynamics of transcription regulation. Biochim Biophys Acta **1819:**657–666. http://dx.doi.org/10.1016/j.bbagrm.2012.03.004.
11. **Bannister AJ, Kouzarides T.** 2011. Regulation of chromatin by histone modifications. Cell Res **21:**381–395. http://dx.doi.org/10.1038/cr.2011.22.
12. **Perissi V, Aggarwal A, Glass CK, Rose DW, Rosenfeld MG.** 2004. A corepressor/coactivator exchange complex required for transcriptional activation by nuclear receptors and other regulated transcription factors. Cell **116:**511–526. http://dx.doi.org/10.1016/S0092-8674(04)00133-3.
13. **Métivier R, Reid G, Gannon F.** 2006. Transcription in four dimensions: nuclear receptor-directed initiation of gene expression. EMBO Rep **7:**161–167. http://dx.doi.org/10.1038/sj.embor.7400626.
14. **Ichiyama K, Yoshida H, Wakabayashi Y, Chinen T, Saeki K, Nakaya M, Takaesu G, Hori S, Yoshimura A, Kobayashi T.** 2008. Foxp3 inhibits RORgammat-mediated IL-17A mRNA transcription through direct interaction with RORgammat. J Biol Chem **283:**17003–17008. http://dx.doi.org/10.1074/jbc.M801286200.
15. **Dignam JD, Lebovitz RM, Roeder RG.** 1983. Accurate transcription initiation by RNA polymerase II in a soluble extract from isolated mammalian nuclei. Nucleic Acids Res **11:**1475–1489. http://dx.doi.org/10.1093/nar/11.5.1475.
16. **Takada I, Tsuji N, Youn MY, Fujiyama S, Okada M, Imai Y, Kondo S, Kitakawa H, Yasuda H, Kato S.** 2010. Purification and identification of estrogen receptor alpha co-regulators in osteoclasts. Ann N Y Acad Sci **1192:**201–207. http://dx.doi.org/10.1111/j.1749-6632.2009.05215.x.
17. **Ichiyama K, Sekiya T, Inoue N, Tamiya T, Kashiwagi I, Kimura A, Morita R, Muto G, Shichita T, Takahashi R, Yoshimura A.** 2011.

Transcription factor Smad-independent T helper 17 cell induction by transforming-growth factor-beta is mediated by suppression of eomesodermin. Immunity **34:**741–754. http://dx.doi.org/10.1016/j.immuni.2011.02.021.

18. **Wakabayashi Y, Tamiya T, Takada I, Fukaya T, Sugiyama Y, Inoue N, Kimura A, Morita R, Kashiwagi I, Takimoto T, Nomura M, Yoshimura A.** 2011. Histone 3 lysine 9 (H3K9) methyltransferase recruitment to the interleukin-2 (IL-2) promoter is a mechanism of suppression of IL-2 transcription by the transforming growth factor-beta-Smad pathway. J Biol Chem **286:**35456–35465. http://dx.doi.org/10.1074/jbc.M111.236794.
19. **Kubo M, Kincaid RL, Webb DR, Ransom JT.** 1994. The $Ca2^{+}$/calmodulin-activated, phosphoprotein phosphatase calcineurin is sufficient for positive transcriptional regulation of the mouse IL-4 gene. Int Immunol **6:**179–188. http://dx.doi.org/10.1093/intimm/6.2.179.
20. **Gong W, Emanuel BS, Galili N, Kim DH, Roe B, Driscoll DA, Budarf ML.** 1997. Structural and mutational analysis of a conserved gene (DGSI) from the minimal DiGeorge syndrome critical region. Hum Mol Genet **6:**267–276. http://dx.doi.org/10.1093/hmg/6.2.267.
21. **Lindsay EA, Rizzu P, Antonacci R, Jurecic V, Delmas-Mata J, Lee CC, Kim UJ, Scambler PJ, Baldini A.** 1996. A transcription map in the CATCH22 critical region: identification, mapping, and ordering of four novel transcripts expressed in heart. Genomics **32:**104–112. http://dx.doi.org/10.1006/geno.1996.0082.
22. **Gennery AR.** 2012. Immunological aspects of 22q11.2 deletion syndrome. Cell Mol Life Sci **69:**17–27. http://dx.doi.org/10.1007/s00018-011-0842-z.
23. **Lindsay EA, Harvey EL, Scambler PJ, Baldini A.** 1998. ES2, a gene deleted in DiGeorge syndrome, encodes a nuclear protein and is expressed during early mouse development, where it shares an expression domain with a Goosecoid-like gene. Hum Mol Genet **7:**629–635. http://dx.doi.org/10.1093/hmg/7.4.629.
24. **Rizzu P, Lindsay EA, Taylor C, O'Donnell H, Levy A, Scambler P, Baldini A.** 1996. Cloning and comparative mapping of a gene from the commonly deleted region of DiGeorge and Velocardiofacial syndromes conserved in C. elegans. Mamm Genome **7:**639–643. http://dx.doi.org/10.1007/s003359900197.
25. **Taricani L, Tejada ML, Young PG.** 2002. The fission yeast ES2 homologue, Bis1, interacts with the Ish1 stress-responsive nuclear envelope protein. J Biol Chem **277:**10562–10572. http://dx.doi.org/10.1074/jbc.M110686200.
26. **Giot L, Bader JS, Brouwer C, Chaudhuri A, Kuang B, Li Y, Hao YL, Ooi CE, Godwin B, Vitols E, Vijayadamodar G, Pochart P, Machineni H, Welsh M, Kong Y, Zerhusen B, Malcolm R, Varrone Z, Collis A, Minto M, Burgess S, McDaniel L, Stimpson E, Spriggs F, Williams J, Neurath K, Ioime N, Agee M, Voss E, Furtak K, Renzulli R, Aanensen N, Carrolla S, Bickelhaupt E, Lazovatsky Y, DaSilva A, Zhong J, Stanyon CA, Finley RL, Jr, White KP, Braverman M, Jarvie T, Gold S, Leach M, Knight J, Shimkets RA, McKenna MP, Chant J, Rothberg JM.** 2003. A protein interaction map of Drosophila melanogaster. Science **302:**1727–1736. http://dx.doi.org/10.1126/science.1090289.
27. **Hegele A, Kamburov A, Grossmann A, Sourlis C, Wowro S, Weimann M, Will CL, Pena V, Luhrmann R, Stelzl U.** 2012. Dynamic protein-protein interaction wiring of the human spliceosome. Mol Cell **45:**567–580. http://dx.doi.org/10.1016/j.molcel.2011.12.034.
28. **Rosenfeld MG, Lunyak VV, Glass CK.** 2006. Sensors and signals: a coactivator/corepressor/epigenetic code for integrating signal-dependent programs of transcriptional response. Genes Dev **20:**1405–1428. http://dx.doi.org/10.1101/gad.1424806.
29. **Cavellán E, Asp P, Percipalle P, Farrants AK.** 2006. The WSTF-SNF2h chromatin remodeling complex interacts with several nuclear proteins in transcription. J Biol Chem **281:**16264–16271. http://dx.doi.org/10.1074/jbc.M600233200.
30. **Barnett C, Krebs JE.** 2011. WSTF does it all: a multifunctional protein in transcription, repair, and replication. Biochem Cell Biol **89:**12–23. http://dx.doi.org/10.1139/O10-114.
31. **Unk I, Hajdu I, Fatyol K, Szakal B, Blastyak A, Bermudez V, Hurwitz J, Prakash L, Prakash S, Haracska L.** 2006. Human SHPRH is a ubiquitin ligase for Mms2-Ubc13-dependent polyubiquitylation of proliferating cell nuclear antigen. Proc Natl Acad Sci U S A **103:**18107–18112. http://dx.doi.org/10.1073/pnas.0608595103.
32. **Romeo Y, Zhang X, Roux PP.** 2012. Regulation and function of the RSK family of protein kinases. Biochem J **441:**553–569. http://dx.doi.org/10.1042/BJ20110289.
33. **Clark DE, Poteet-Smith CE, Smith JA, Lannigan DA.** 2001. Rsk2 allosterically activates estrogen receptor alpha by docking to the hormone-binding domain. EMBO J **20:**3484–3494. http://dx.doi.org/10.1093/emboj/20.13.3484.
34. **Huang ZM, Wu J, Jia ZC, Tian Y, Tang J, Tang Y, Wang Y, Wu YZ, Ni B.** 2012. Identification of interacting proteins of retinoid-related orphan nuclear receptor gamma in HepG2 cells. BMB Rep **45:**331–336. http://dx.doi.org/10.5483/BMBRep.2012.45.6.249.
35. **Mudter J, Yu J, Zufferey C, Brustle A, Wirtz S, Weigmann B, Hoffman A, Schenk M, Galle PR, Lehr HA, Mueller C, Lohoff M, Neurath MF.** 2011. IRF4 regulates IL-17A promoter activity and controls RORgammat-dependent T_H17 colitis in vivo. Inflamm Bowel Dis **17:**1343–1358. http://dx.doi.org/10.1002/ibd.21476.
36. **Zhang F, Meng G, Strober W.** 2008. Interactions among the transcription factors Runx1, RORgammat and Foxp3 regulate the differentiation of interleukin 17-producing T cells. Nat Immunol **9:**1297–1306. http://dx.doi.org/10.1038/ni.1663.
37. **Gomez-Rodriguez J, Sahu N, Handon R, Davidson TS, Anderson SM, Kirby MR, August A, Schwartzberg PL.** 2009. Differential expression of interleukin-17A and -17F is coupled to T cell receptor signaling via inducible T cell kinase. Immunity **31:**587–597. http://dx.doi.org/10.1016/j.immuni.2009.07.009.
38. **Chen Z, Laurence A, Kanno Y, Pacher-Zavisin M, Zhu BM, Tato C, Yoshimura A, Hennighausen L, O'Shea JJ.** 2006. Selective regulatory function of Socs3 in the formation of IL-17-secreting T cells. Proc Natl Acad Sci U S A **103:**8137–8142. http://dx.doi.org/10.1073/pnas.0600666103.
39. **Lin JX, Spolski R, Leonard WJ.** 2008. Critical role for Rsk2 in T-lymphocyte activation. Blood **111:**525–533. http://dx.doi.org/10.1182/blood-2007-02-072207.
40. **Ashe A, Morgan DK, Whitelaw NC, Bruxner TJ, Vickaryous NK, Cox LL, Butterfield NC, Wicking C, Blewitt ME, Wilkins SJ, Anderson GJ, Cox TC, Whitelaw E.** 2008. A genome-wide screen for modifiers of transgene variegation identifies genes with critical roles in development. Genome Biol **9:**R182. http://dx.doi.org/10.1186/gb-2008-9-12-r182.
41. **Sapkota GP, Cummings L, Newell FS, Armstrong C, Bain J, Frodin M, Grauert M, Hoffmann M, Schnapp G, Steegmaier M, Cohen P, Alessi DR.** 2007. BI-D1870 is a specific inhibitor of the p90 RSK (ribosomal S6 kinase) isoforms in vitro and in vivo. Biochem J **401:**29–38. http://dx.doi.org/10.1042/BJ20061088.